

CHAPTER 6

STABILITY AND FAILURE OF SUDDENLY LOADED LAMINATED COMPOSITE CYLINDRICAL PANEL WITH CUTOUT

6.1 Introduction

After the investigation of stability and failure of a laminated composite cylindrical panel in the previous chapter, in this chapter, the stability and failure of a laminated composite cylindrical panel with centrally placed cutout subjected to in-plane pulse load are investigated. The influence of loading duration, loading function, cutout geometry and the stacking sequence on the dynamic buckling behaviour is checked. Before the results of the present study, the results of the convergence and validation study are presented. The chapter is divided into the following subsections:

- Convergence and Validation Studies
 - Convergence and Validation of Static Buckling Load of a Plate with Cutout
 - Validation of Static Buckling Load of a Composite Plate with Cutout
 - Validation of Natural Frequency of a Cylindrical Panel with Cutout
- Dynamic Buckling Studies
 - Effect of Loading Duration
 - Failure of Cylindrical Panel with a Cutout
 - Effect of Loading Function
 - Effect of Curvature
 - Effect of Size of the Cutout
 - Effect of the Shape of the Cutout
 - Deformation of a Cylindrical Panel with a Cutout

6.2 Convergence and Validation Studies

In this section, the results of the convergence and validation study of an isotropic plate with cutout, laminated composite plate with cutout and isotropic cylindrical panel with cutout are presented.

6.2.1 Convergence and validation of static buckling load of a plate with cutout

The static buckling load of a plate is calculated and compared with the results from the existing literature. The plate dimensions are $a=b=20\text{in.}$, $h=0.1\text{in.}$ with a square cutout (c -cutout side) at the centre of the plate. The material properties are $E=16\times 10^6\text{ lb/in}^2$, $G=6.2\times 10^6\text{ lb/in}^2$ and $\nu=0.3$. Figure 6.1(a) shows the geometry of the plate. Figure 6.1(b) shows the pre-buckling boundary conditions and Fig. 6.1(c) shows the buckling boundary conditions. Figure 6.2 shows the results of the convergence study with static buckling load (lb/in) for a plate without cutout ($c/a=0$) for various mesh sizes. Table 6.1 shows the results of the present study with the finite element results of Ko (1998) and Patel *et al.* (2010).

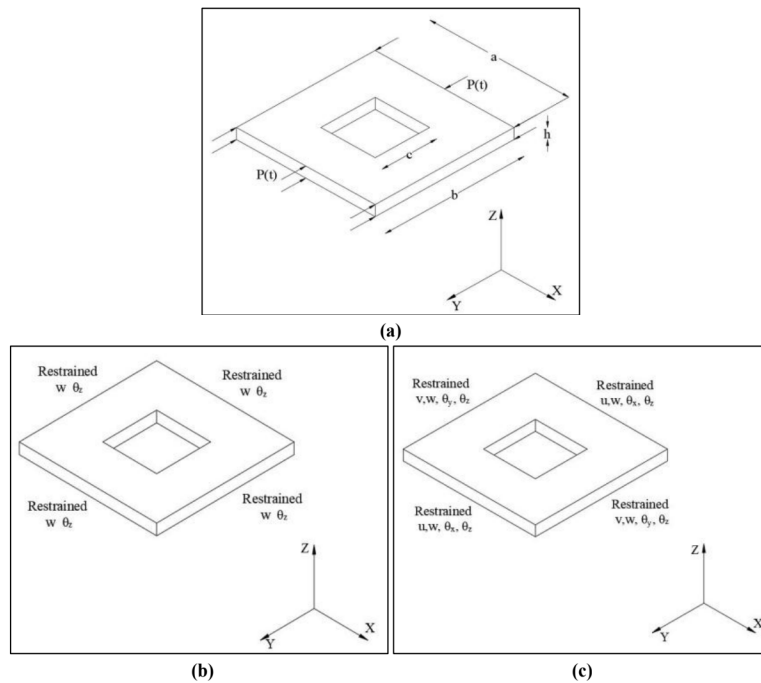


Fig. 6.1 Plate with a square cutout for validation study (a) Geometry (b) Pre-buckling boundary conditions (c) Buckling boundary conditions

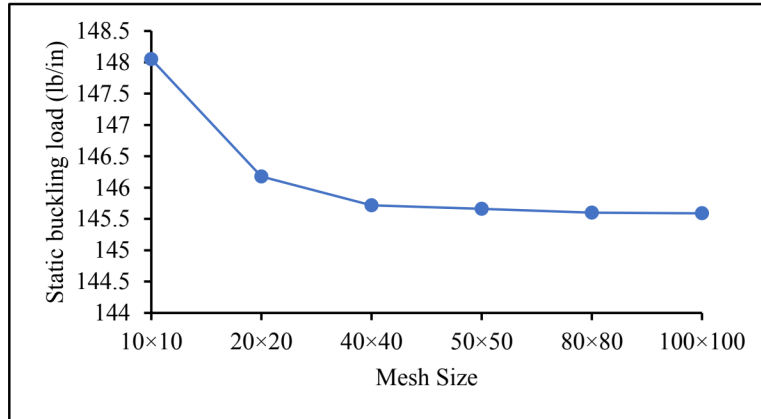


Fig. 6.2 Plot of static buckling load vs Mesh size of a plate with cutout

Table 6.1 Static buckling load for an isotropic square plate with a central square cutout for various length of cutout side to length of plate ratios

Analysis	Static buckling load (lb/in)			
	$c/b=0$	$c/b=0.2$	$c/b=0.4$	$c/b=0.6$
Present	145.66	125	109.29	103.48
Ko (1998)	144.8	126.3	107	100.6
Patel <i>et al.</i> (2010)	146.157	127.551	110.424	103.786
Error (%)	0.59	1.03	2.14	2.86

From Fig. 6.2, it is seen that the mesh size of 50×50 is converged. From Table 6.1 it is seen that the result of the present study match with the results from the literature. The error shown in the table is with respect to the results reported by Ko (1998) which in all cases is lower than 3%.

6.2.2 Validation of static buckling load for a composite plate with cutout

In this section, the results of the static buckling load of the present study are compared with the results for the available literature. A simply supported square plate with $a=b=20$ in, $h=0.064$ in and material properties $E_L=27.72 \times 10^6$ lb/in², $E_T=18.09 \times 10^6$ lb/in², $G_{LT}=8.15 \times 10^6$ lb/in², $\nu=0.3$ is considered. The lamination scheme is $[90/0/0/90]_2$. The boundary conditions are shown in Fig. 6.1(b) and Fig. 6.1(c). The results from the current study are compared with the finite element method results of Ko (1998) in Table 6.2.

Table 6.2. Static buckling load for a laminated composite square plate with a central square cutout for various ratios of cutout side to length of the plate.

Analysis	Static buckling load (lb/in)				
	<i>c/b</i> =0.1	<i>c/b</i> =0.2	<i>c/b</i> =0.3	<i>c/b</i> =0.4	<i>c/b</i> =0.5
Ko (1998)	46.945	42.839	39.685	37.725	36.490
Present	47.741	43.553	40.376	38.419	37.209
Error (%)	1.69	1.66	1.74	1.84	1.97

It is seen from Table 6.2 that the results of the present study match with the results from the literature. The error percentage for all cases is lower than 2.

The results of the static buckling load of a composite plate with cutout has also been validated with the experimental and finite element results of Baba and Baltaci (2007). Plate with $E_{11}=39\text{GPa}$, $E_{22}=8.2\text{GPa}$, $G_{12}=G_{23}=G_{13}=2.9\text{GPa}$ and $\nu_{12}=0.29$ is considered. The stacking sequence is $(90^\circ/45^\circ/-45^\circ/0^\circ)_s$. The geometric properties are $a=25\text{mm}$, $b=150\text{mm}$, $h=2\text{mm}$ and the diameter of the circular cutout at the centre =5mm. Two unloaded edges are free, and the other edges are clamped. Table 6.3 shows the results of the present study compared with the finite element method results and the experimental results of Baba and Baltaci (2007). The error is shown in parenthesis in Table 6.3 is with respect to the experimental result of Baba and Baltaci (2007). It is seen that the results of the present study match well with the results from Baba and Baltaci (2007).

Table 6.3 Static buckling load for a laminated composite rectangular plate with stacking sequence is $(90^\circ/45^\circ/-45^\circ/0^\circ)_s$ and a central circular cutout.

	Baba and Baltaci, 2007		Present
	Experimental	FEM	
Plate without cutout	382	397.5	396.1
		(4.06)	(3.69)
Plate with circular cutout	410	377.4	378.5
		(7.95)	(7.68)

6.2.3 Validation of natural frequency of a cylindrical panel with cutout

In this section, the natural frequency of a cylindrical panel is validated. The geometric properties of the panel are $a=b=500\text{mm}$, $h=2\text{mm}$, $R=2000$. The material properties are

$E=7020\text{kg/mm}^2$, $\rho=2.72\times 10^{-10}\text{ kg-s}^2/\text{mm}^4$ and $\nu=0.3$. The geometry of the cylindrical panel is shown in Fig 6.3(a). The cylindrical panel is clamped on all four sides as shown in Fig. 6.3(b). The results of the present study are compared with finite element results of Sivasubramonian *et al.* (1999) and Sahu and Datta (2002) and presented in Table 6.4. The error is presented in parenthesis in Table 6.4 is with respect to the results from Sivasubramonian *et al.* (1999).

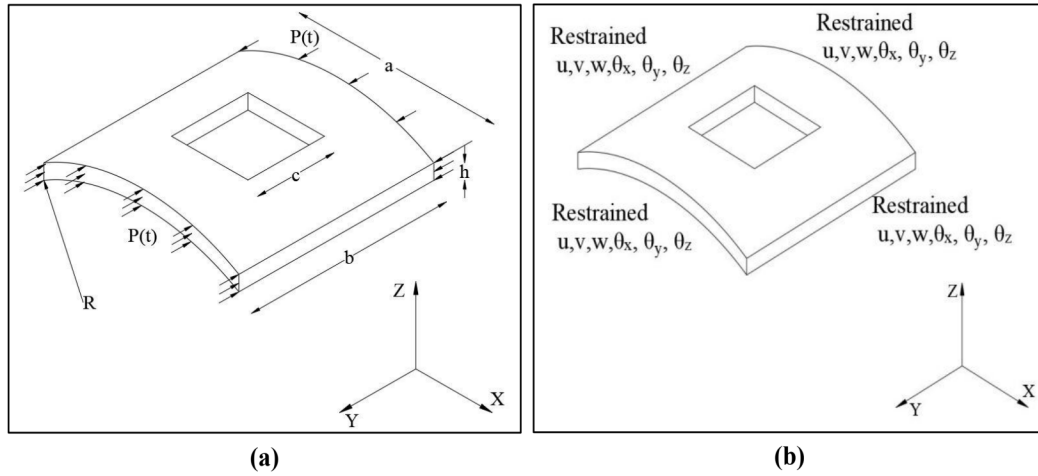


Fig. 6.3 Cylindrical panel with central cutout for the validation study (a) Geometry (b) boundary conditions

Table 6.4 Natural frequency for a cylindrical panel with central square cutout for various length of cutout side to length of panel ratios.

	Sivasubramonian <i>et al.</i> (1999)	Sahu and Datta (2002)	Present
$c/b=0$	213.9	215.23 (0.62)	217.52 (1.69)
$c/b=0.5$	185.3	184.73 (0.31)	185.02 (0.15)

It is seen from Table 6.4 that the results of the current study match with the results from the literature.

From the convergence and validation studies, the results of the present study with a mesh size of 50×50 on all four edges match well with the results from the literature. The same mesh size is used for the rest of the study. For the case of boundary conditions, same boundary

conditions for both pre-buckling and buckling stages are considered as done in the previous chapter.

6.3 Dynamic Buckling Studies

In this section, the results for the current investigation are presented. The influence of loading duration, curvature, cutout size and cutout geometry on the dynamic buckling behavior of laminated composite cylindrical panels are investigated. The geometry of the panel is presented in Fig. 3.8(a). Simply supported boundary conditions are presented in Fig. 3.8(b). The circular, square and square-rotated cutouts are presented in Fig. 3.9(a) - 3.9(c) respectively. The material properties presented in Table 3.2 are considered. The procedure for calculating the dynamic buckling load and the first ply failure load are the same as presented in section 4.3.

Due the presence of the cutout of different area and geometry, the static buckling load of the panel changes. In each section, the value of N_{st} for each case is different. So, the dynamic performance of the panel is evaluated with respect to its static buckling load. The static buckling load and the first natural period of the cylindrical panel considered in the investigation are presented in Table 6.5. The geometric properties of the panel are: $b/a=1$, $b/h=100$ with $a=0.1$ m with various radius of curvatures and stacking schemes.

Table 6.5 Static buckling load and first natural period of the cylindrical panel with cutout having $b/a=1$, $b/h=100$ with $b=0.1$ m with various radius of curvatures and stacking schemes.

R/a	Stacking Scheme	Cutout Shape	Cutout area (%)	Static Buckling Load (N/m)	First Natural Period (s)
20	(0°/90°/90°/0°)	Circular	5	11953	2.27×10^{-3}
20	(0°/90°/90°/0°)	Circular	10	9914	2.07×10^{-3}
20	(0°/90°/90°/0°)	Circular	20	7841	2.24×10^{-3}
10	(0°/90°/90°/0°)	Circular	5	14695	1.98×10^{-3}
10	(0°/90°/90°/0°)	Circular	10	11991	1.99×10^{-3}
10	(0°/90°/90°/0°)	Circular	20	8911	1.91×10^{-3}
5	(0°/90°/90°/0°)	Circular	5	23068	1.43×10^{-3}
5	(0°/90°/90°/0°)	Circular	10	17079	1.41×10^{-3}
5	(0°/90°/90°/0°)	Circular	20	10880	1.34×10^{-3}
20	(45°/-45°/-45°/45°)	Circular	5	28403	1.69×10^{-3}

(Table 6.5 Continued)

20	(45°/-45°/-45°/45°)	Circular	10	24945	1.64×10 ⁻³
20	(45°/-45°/-45°/45°)	Circular	20	21389	1.45×10 ⁻³
10	(45°/-45°/-45°/45°)	Circular	5	31691	1.38×10 ⁻³
10	(45°/-45°/-45°/45°)	Circular	10	26123	1.38×10 ⁻³
10	(45°/-45°/-45°/45°)	Circular	20	20705	1.30×10 ⁻³
5	(45°/-45°/-45°/45°)	Circular	5	36061	9.02×10 ⁻⁴
5	(45°/-45°/-45°/45°)	Circular	10	29243	9.45×10 ⁻⁴
5	(45°/-45°/-45°/45°)	Circular	20	20212	9.84×10 ⁻⁴
10	(0°/90°/90°/0°)	Square	5	14792	1.98×10 ⁻³
10	(0°/90°/90°/0°)	Square	10	11961	2.00×10 ⁻³
10	(0°/90°/90°/0°)	Square	20	8562	1.94×10 ⁻³
10	(45°/-45°/-45°/45°)	Square	5	30843	1.43×10 ⁻³
10	(45°/-45°/-45°/45°)	Square	10	25748	1.47×10 ⁻³
10	(45°/-45°/-45°/45°)	Square	20	21371	1.41×10 ⁻³
10	(0°/90°/90°/0°)	Square-rotated	5	14054	2.06×10 ⁻³
10	(0°/90°/90°/0°)	Square-rotated	10	11332	2.12×10 ⁻³
10	(0°/90°/90°/0°)	Square-rotated	20	8512	2.14×10 ⁻³
10	(45°/-45°/-45°/45°)	Square-rotated	5	31451	1.39×10 ⁻³
10	(45°/-45°/-45°/45°)	Square-rotated	10	25599	1.40×10 ⁻³
10	(45°/-45°/-45°/45°)	Square-rotated	20	19711	1.34×10 ⁻³
20	(0°/90°/90°/0°)	No Cutout	-	15238	2.08×10 ⁻³
10	(0°/90°/90°/0°)	No Cutout	-	18212	1.9×10 ⁻³
5	(0°/90°/90°/0°)	No Cutout	-	30848	1.41×10 ⁻³
20	(45°/-45°/-45°/45°)	No Cutout	-	29975	1.66×10 ⁻³
10	(45°/-45°/-45°/45°)	No Cutout	-	30949	1.32×10 ⁻³
5	(45°/-45°/-45°/45°)	No Cutout	-	45934	8.41×10 ⁻⁴

6.3.1 Effect of loading duration

In this section, the effect of loading duration is studied. For study, laminated composite cylindrical panel with $R/a=10$, $b/a=1$, $b/h=100$ and stacking sequence (0°/90°/90°/0°) is

considered. Two circular cutout areas are considered 5% and 20%. The duration of loadings (T_b) considered are $0.25T_n$, $0.5T_n$, T_n , $2.5T_n$ and $5T_n$. The panel is subjected to a rectangular pulse load. Figure 6.4(a) shows the plot of non-dimensional load vs non-dimensional displacement for various durations of loading for panel with 5% cutout area and Fig. 6.4(b) shows the plot of non-dimensional load vs non-dimensional displacement for various durations of loading for panel with 20% cutout area.

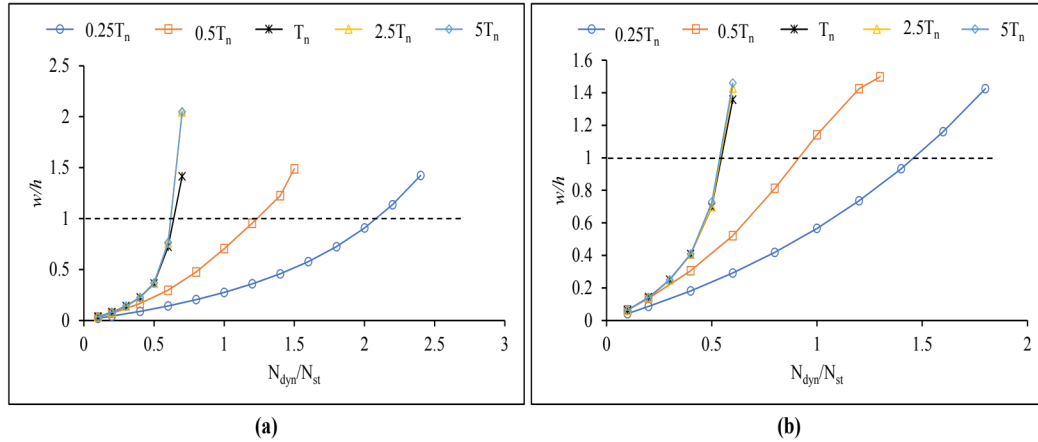


Fig. 6.4 Non-dimensional Load vs non-dimensional Displacement for a panel with $R/a=10$, stacking sequence $(0^\circ/90^\circ/90^\circ/0^\circ)$ for various durations of rectangular pulse loading (a) 5% circular cutout area at the centre (b) 20% circular cutout area at the centre

The value is N_{st} in Fig. 6.4(a) is different from the panel in in Fig. 6.4(b). Also, the first natural periods are also different. Thus, the dynamic performance of the panel with 5% cutout and 20% cutout are different. The dynamic buckling load of the panel with 5% cutout and subjected to a rectangular pulse load till its first natural period is 35% lower than its static buckling load and that of the panel with 20% cutout it is 48% lower. These results show that the stiffness of the panel with cutout when subjected in-plane pulse loads is much lower than that of the panel when subjected to static in-plane loads. It is observed from Fig. 6.4(a) and Fig. 6.4(b) that the responses start to converge if the duration of loading is greater than the first natural period. This shows that the fundamental first natural period is the critical loading duration in the laminated composite cylindrical panel with cutout. It is also observed that when the loading duration is equal to and higher than the first natural period, the dynamic buckling load for cylindrical panel with cutout are 5% or 20% is lower than the respective static buckling load. Thus, the stiffness of the panel changes with the change in duration of loading and also

the area of circular cutout. For the rest of the study, the duration of loading kept as the first natural period of the cylindrical panel considered.

6.3.2 Failure of the cylindrical panel with cutout

In this section, the first ply failure of a laminated composite cylindrical panel with cutout is studied. For this study, cylindrical panel with geometry $R/a=10$, $b/a=1$, $b/h=100$ and stacking sequence $(0^\circ/90^\circ/90^\circ/0^\circ)$ is considered. The area of the central circular cutout is 10%. The panel is subjected to rectangular pulse load till its first natural period.

Figure 6.5(a) shows the plot of non-dimensional load vs non-dimensional displacement for panel with 10% cutout area and Fig. 6.5(b) shows the plot of non-dimensional load vs Failure Index with respect to various failure theories for panel with 10% cutout area. The first ply failure occurs at $N_{dyn}/N_{st}=0.8$ (Fig. 6.5(b)). The failure index is maximum at node 15 which is near the cutout. The failure index at layer 1 is 1.0433, at layer 2 is 0.2654 at layer 3 is 0.1967 and at layer 4 is 0.8948. Figure 6.6(a) shows the deformed shape of the panel showing the maximum transverse displacement at the centre at $N_{dyn}/N_{st} = 0.6$. Figure 6.6(b) shows the deformed shape of the panel showing the maximum failure index with respect to Tsai-Wu failure criterion at $N_{dyn}/N_{st} = 0.6$. Figure 6.6(c) shows the deformed shape of the panel showing the maximum transverse displacement at the centre of the panel at $N_{dyn}/N_{st} = 0.8$. Figure 6.6(d) shows the deformed shape of the panel showing the maximum failure index with respect to Tsai-Wu failure criterion. at $N_{dyn}/N_{st} = 0.8$. In Fig. 6.6(a)-6.6(d), the panel with $R/a=10$, stacking sequence $(0^\circ/90^\circ/90^\circ/0^\circ)$ and 10% circular cutout area are considered. The scale factor for these figures is 10.

It is observed from Fig. 6.5(a) that the dynamic buckling load is lower than the static buckling load (40% lower) for the cylindrical panel with 10% cutout area. From Fig. 6.5(b) it is seen that the failure index for all the four failure criteria are very close to each other. However, it is to be mentioned that the values are not the same and some differences are present. The first ply failure load of the panel with respect to Tsai-Wu criterion is 25% lower than its static buckling load. The strength and the stiffness of the panel with cross-ply laminates, 10% circular cutout area at the center and subjected to in-plane rectangular pulse load is much lower than the panel when subjected to static in-plane load. The blue regions in Fig. 6.6(a) and Fig. 6.6(c) represent regions of maximum deformation. The red region in Fig. 6.6(b) and Fig.

6.6(d) show the region of maximum failure index in Tsai-Wu failure criterion. The failure index is calculated at each node. The node with the maximum failure index in the region is taken into consideration. It is observed that the failure occurs in a region around the cutout. It is also observed that the non-linear dynamic buckling occurs before first ply failure of the laminated composite cylindrical panel with cutout.

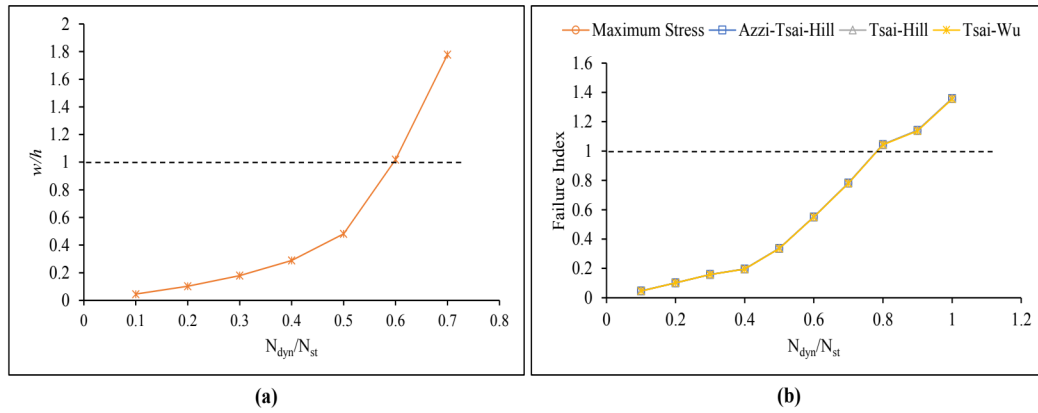


Fig. 6.5 Plot for a panel with $R/a=10$, stacking sequence $(0^\circ/90^\circ/90^\circ/0^\circ)$ and 10% circular cutout area subjected to rectangular pulse load **(a)** Non-dimensional Load vs non-dimensional Displacement **(b)** Non-dimensional Load vs Failure index

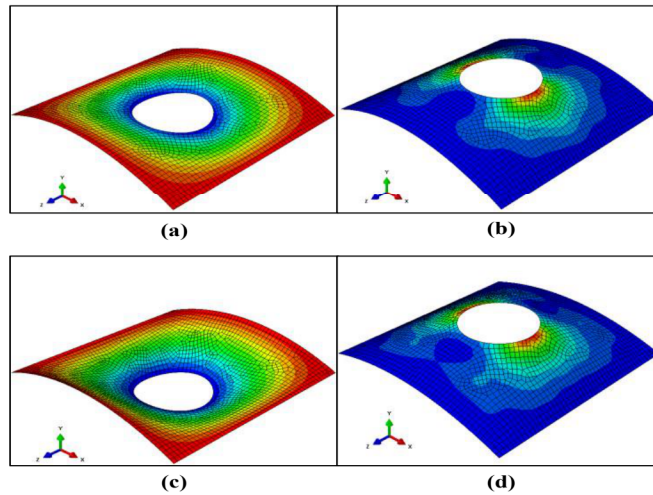


Fig. 6.6 Deformed shape of the panel with $R/a=10$, stacking sequence $(0^\circ/90^\circ/90^\circ/0^\circ)$ and 10% circular cutout area. Scale factor=10. **(a)** $N_{dyn}/N_{st} = 0.6$ showing the maximum transverse displacement **(b)** $N_{dyn}/N_{st} = 0.6$ showing the Tsai-Wu Failure Criterion **(c)** $N_{dyn}/N_{st} = 0.8$ showing the maximum transverse displacement **(d)** $N_{dyn}/N_{st} = 0.8$ showing the Tsai-Wu Failure Criterion.

6.3.3 Effect of loading function

In this section, the results of effect of loading function are discussed. The geometric properties are taken as, $R/a=10$, $b/a=1$, $b/h=100$ and stacking sequence is $(0^\circ/90^\circ/90^\circ/0^\circ)$. The cutout areas are 5% and 10%. The panel is subjected to rectangular and sinusoidal pulse loads.

Figure 6.7(a) shows the plot of non-dimensional load vs non-dimensional displacement for panel with stacking sequence is $(0^\circ/90^\circ/90^\circ/0^\circ)$ for two pulse loading functions. Figure 6.7(b) shows the plot of non-dimensional load vs failure index for panel with stacking sequence is $(0^\circ/90^\circ/90^\circ/0^\circ)$ for two pulse loading functions. In Fig. 6.7(a) and Fig. 6.7(b), R5 represents rectangular pulse load on the panel with 5% cutout area, S5 represents sinusoidal pulse load on the panel with 5% cutout area, R10 represents rectangular pulse load on the panel with 10% cutout area and S10 represents sinusoidal pulse load on the panel with 10% cutout area. Also, R0 and S0 represent the panel without cutouts subjected to rectangular and sinusoidal pulse loads respectively. In Fig. 6.7(a) and Fig. 6.7(b), solid lines represent rectangular pulse load and dash lines represent sinusoidal pulse loads.

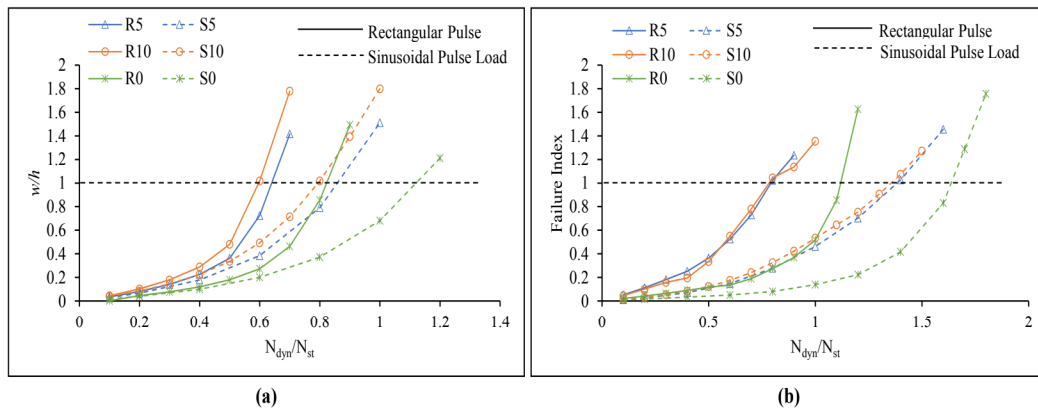


Fig.6.7 Plot for a panel with $R/a=10$, $b/a=1$, $b/h=100$ and stacking sequence $(0^\circ/90^\circ/90^\circ/0^\circ)$ for various loading functions and central cutout areas **(a)** Non-dimensional Load vs non-dimensional Displacement **(b)** Non-dimensional Load vs Failure index (Tsai-Wu criterion)

With the change in size of the cutout, the value of N_{st} changes in Fig. 6.7(a) and Fig. 6.7(b). In Fig. 6.7(b), the plots for panel with 5% and 10% cutout and subjected to either rectangular pulse load are over lapping. However, the value of N_{st} is different in each case. The dynamic performance of the panel when subjected to rectangular loading function is lower than the panel

when subjected to sinusoidal loading function. The panel with cutout when subjected to sinusoidal loading function has dynamic buckling load 20%-24% lower than its respective static buckling load. The panel with cutout when subjected to rectangular loading function has dynamic buckling load 36%-40% lower than its respective static buckling load. However, the panel when subjected to sinusoidal loading function has first ply failure load higher than its respective static buckling load in all cases. This signifies that the strength and the stiffness of the panel changes with the change in loading function. The strength of the panel when subjected to sinusoidal in-plane pulse load is higher than the panel when subjected to rectangular in-panel pulse load.

6.3.4 Effect of curvature

In this section, the effect of curvature on the nonlinear dynamic buckling of laminated composite cylindrical panel is studied. The geometric properties are $b/a=1$, $b/h=100$ and stacking sequence is $(0^\circ/90^\circ/90^\circ/0^\circ)$. The curvatures considered are: $R/a=5$, 10 and 20. The central circular cutout areas are 5% and 10%.

Figure 6.8(a) shows the plot of non-dimensional load vs non-dimensional displacement for a panel with 5% circular cutout area for various radius of curvatures. Figure 6.8(b) shows the plot of non-dimensional load vs failure Index (Tsai-Wu failure criterion) for a panel with 5% circular cutout area for various radius of curvatures. Figure 6.9(a) shows the plot of non-dimensional load vs non-dimensional displacement for a panel with 10% circular cutout area for various radius of curvatures. Figure 6.9(b) shows the plot of non-dimensional load vs failure index (Tsai-Wu failure criterion) for panel with 10% circular cutout area for various radius of curvatures. In Fig. 6.8 and Fig. 6.9, solid lines represent panel with cutout and dash lines represent panel without cutout.

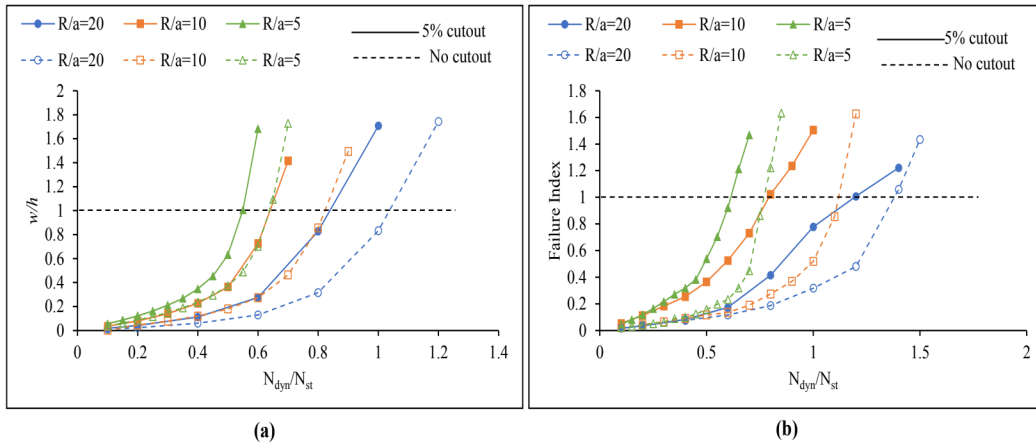


Fig. 6.8 Plot for a panel with $b/a=1$, $b/h=100$, stacking sequence $(0^\circ/90^\circ/90^\circ/0^\circ)$, subjected to rectangular pulse load and 5% circular cutout area for various radius of curvatures **(a)** Non-dimensional Load vs non-dimensional Displacement **(b)** Non-dimensional Load vs Failure Index (Tsai-Wu criterion)

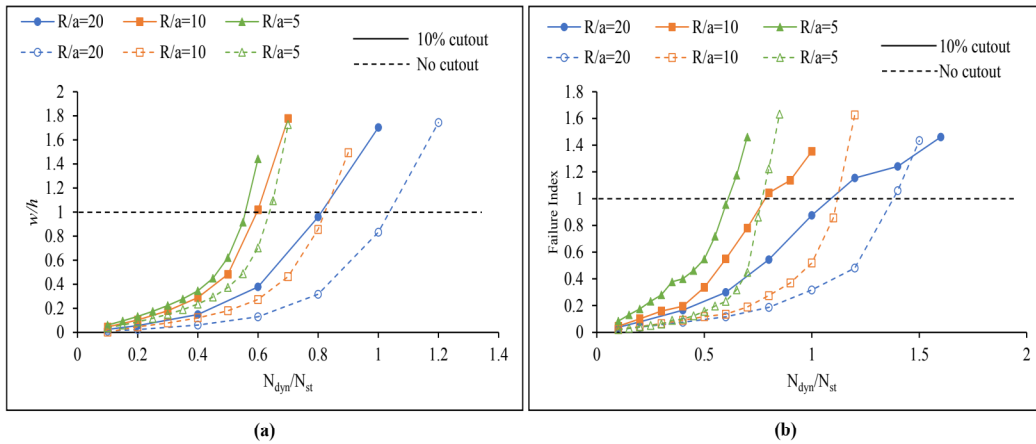


Fig. 6.9 Plot for a panel with $b/a=1$, $b/h=100$, stacking sequence $(0^\circ/90^\circ/90^\circ/0^\circ)$, subjected to rectangular pulse load and 10% circular cutout area for various radius of curvatures. **(a)** Non-dimensional Load vs non-dimensional Displacement **(b)** Non-dimensional Load vs Failure Index (Tsai-Wu criterion)

In Fig. 6.8 and Fig. 6.9, the with the change in the curvature of the panel, the static buckling load of the panel (N_{st}) changes. In Fig. 6.8(a) the plots for the panel with $R/a=10$ and $R/a=5$ with 5% cutout and without cutout merge. However, the dynamic buckling loads are different in both cases which are 36% lower than their respective static buckling loads. It is observed from Fig. 6.8(a) and 6.9(a) that the dynamic buckling loads of the panels with 5% or 10% cutouts have lower stiffness than the panels without cutouts. In all the cases of the curvatures

considered, the dynamic buckling load of the panels with cutouts are lower than their respective static buckling loads. However, in Fig. 6.8(b) and 6.9(b) it is observed that the first ply failure of the panel with $R/a=20$ has first ply failure load higher than its static buckling load and for the panels with higher curvatures, the first ply failure loads are lower than their respective static buckling load. For the panel with $R/a=20$ and 5% circular cutout, its dynamic buckling load is 16% lower than its static buckling load and with the same curvature and 10% cutout area, it is 19% lower than its static buckling load. These results show that the panel with lower curvature exhibits higher stiffness when subjected to rectangular in-plane pulse load till its first natural period than the panel with higher curvature.

6.3.5 Effect of size of the cutout

In this section, the effect of size of the central circular cutout on the stability and failure of a composite cylindrical panel subjected to pulse load is studied. The cylindrical panel with $b/a=1$, $b/h=100$ is considered. The curvatures $R/a=10$ and $R/a=5$ are considered. The stacking sequences considered are $(0^\circ/90^\circ/90^\circ/0^\circ)$ and $(45^\circ/-45^\circ/-45^\circ/45^\circ)$.

Figure 6.10(a) shows the plot of non-dimensional load vs non-dimensional displacement for a panel with $R/a=10$ and stacking sequence $(0^\circ/90^\circ/90^\circ/0^\circ)$, for various cutout areas. Figure 6.10(b) shows the plot of non-dimensional load vs failure index for a panel with $R/a=10$ and stacking sequence $(0^\circ/90^\circ/90^\circ/0^\circ)$, for various cutout areas. Figure 6.10(c) shows the plot of non-dimensional load vs non-dimensional displacement for panel with $R/a=5$ and stacking sequence $(0^\circ/90^\circ/90^\circ/0^\circ)$, for various cutout areas. Figure 6.10(d) shows the plot of non-dimensional load vs failure index for a panel with $R/a=5$ and stacking sequence $(0^\circ/90^\circ/90^\circ/0^\circ)$, for various cutout areas.

Figure 6.11(a) shows the plot of non-dimensional load vs non-dimensional displacement for a panel with $R/a=10$ and stacking sequence $(45^\circ/-45^\circ/-45^\circ/45^\circ)$, for various cutout areas. Figure 6.11(b) shows the plot of non-dimensional load vs failure index for a panel with $R/a=10$ and stacking sequence $(45^\circ/-45^\circ/-45^\circ/45^\circ)$, for various cutout areas. Figure 6.11(c) shows the plot of non-dimensional load vs non-dimensional displacement for a panel with $R/a=5$ and stacking sequence $(45^\circ/-45^\circ/-45^\circ/45^\circ)$, for various cutout areas. Figure 6.11(d) shows the plot of non-dimensional load vs failure index for a panel with $R/a=5$ stacking sequence $(45^\circ/-45^\circ/-45^\circ/45^\circ)$,

for various cutout areas. In Fig. 6.10 and Fig. 6.11, the panel is subjected to rectangular pulse load till its first natural period. Also, 0% cutout area represents panel without cutout.

In Fig. 6.10 and 6.11, with the change in the area of the cutout, the static buckling load of the panel (N_{st}) changes. Also, with the change in the stacking scheme of the laminates, the value of N_{st} changes. In Fig. 6.10(a) panel with cross-ply laminates and $R/a=10$ having 5%, 10% and 20% circular cutout area, the dynamic buckling loads are 36%, 40% and 46% lower than their respective static buckling loads. In Fig. 6.10(c) panel with cross-ply laminates and $R/a=5$ having 5%, 10% and 20% circular cutout area, the dynamic buckling loads are 46%, 44% and 43% lower than their respective static buckling loads. Similarly, in Fig. 6.10(b) panel with cross-ply laminates and $R/a=10$ having 5%, 10% and 20% circular cutout area, the first ply failure loads are 21%, 22% and 26% lower than their respective static buckling loads. In Fig. 6.10(d) panel with cross-ply laminates and $R/a=5$ having 5%, 10% and 20% circular cutout area, the first ply failure loads are 38%, 38% and 35% lower than their respective static buckling loads.

In Fig. 6.11(a) panel with angle-ply laminates and $R/a=10$ having 5%, 10% and 20% circular cutout area, the dynamic buckling loads are 60%, 57% and 52% lower than their respective static buckling loads. In Fig. 6.11(c) panel with angle-ply laminates and $R/a=5$ having 5%, 10% and 20% circular cutout area, the dynamic buckling loads are 57%, 56% and 55% lower than their respective static buckling loads. Similarly, in Fig. 6.11(b) panel with angle-ply laminates and $R/a=10$ having 5%, 10% and 20% circular cutout area, the first ply failure loads are 55%, 52% and 44% lower than their respective static buckling loads. In Fig. 6.11(d) panel with angle-ply laminates and $R/a=5$ having 5%, 10% and 20% circular cutout area, the first ply failure loads are 51%, 52% and 50% lower than their respective static buckling loads.

The dynamic buckling load of the panel with circular cutout having $R/a=10$ exhibit different stiffness when subjected to rectangular in-plane pulse load than the panel with $R/a=5$. This is observed in both cross-ply and angle-ply laminates. With the change in the curvature of the panel, the stiffness of the panel the strains generated in the panels vary. Due to the presence of a cutout, the strains generated in the panel when subjected to in-plane pulse loads affect the maximum deflection in the panel. This could be the reason why a variation in performance of the panel with is cutout is observed when subjected to in-plane pulse loads till their first natural periods.

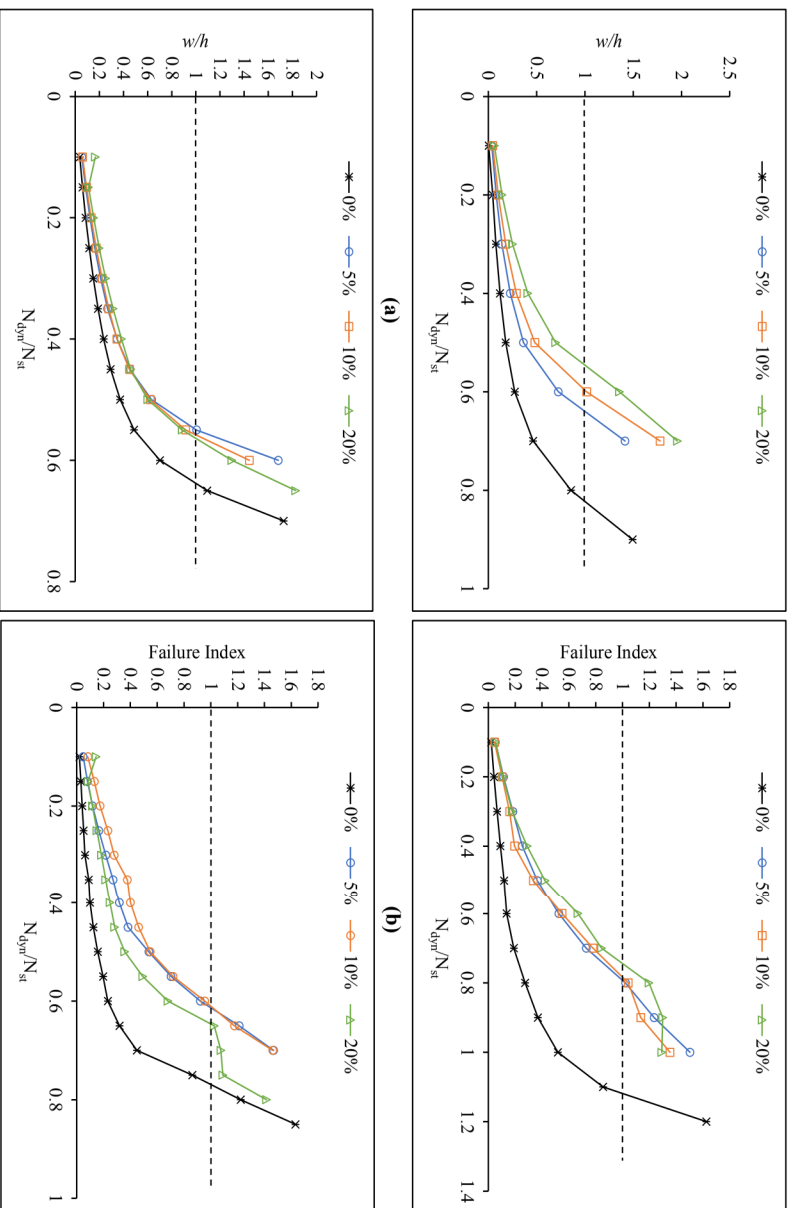


Fig. 6.10 Plot for a cylindrical panel with $b/a=1$, $b/h=100$ and stacking sequence ($0^\circ/90^\circ/90^\circ/0^\circ$) for various cutout areas subjected to rectangular pulse load **(a)** Non-dimensional Load vs non-dimensional Displacement for panel with $R/a=10$, **(b)** Non-dimensional Load vs Failure Index (Tsai-Wu criterion) for panel with $R/a=10$ **(c)** Non-dimensional Load vs non-dimensional Displacement for panel with $R/a=5$, **(d)** Non-dimensional Load vs Failure Index (Tsai-Wu criterion) for panel with $R/a=5$

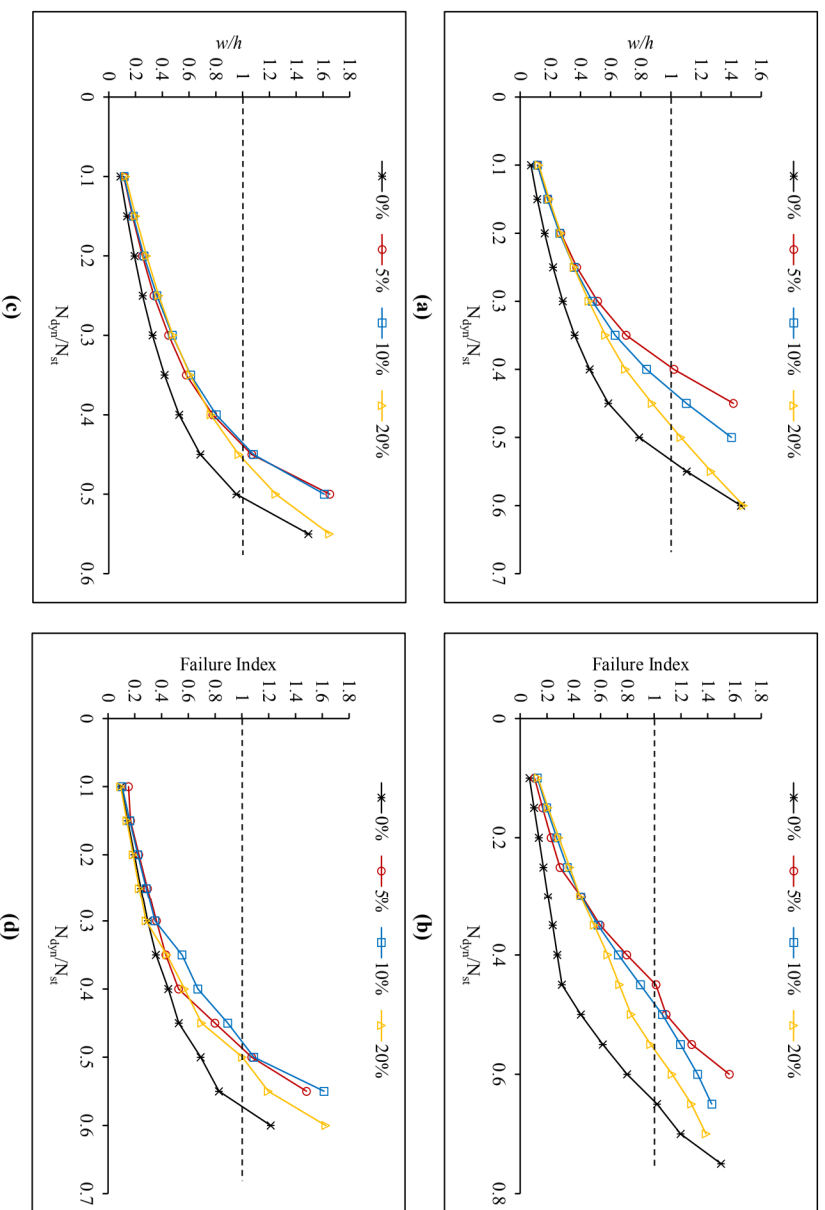


Fig. 6.11 Plot for a cylindrical panel with $b/a=1$, $b/h=100$ and stacking sequence $(45^\circ/-45^\circ/-45^\circ/45^\circ)$ for various cutout areas subjected to rectangular pulse load **(a)** Non-dimensional Load vs non-dimensional Displacement for panel with $R/a = 10$, **(b)** Non-dimensional Load vs Failure Index (Tsai-Wu criterion) for panel with $R/a = 10$ **(c)** Non-dimensional Load vs non-dimensional Displacement for panel with $R/a = 5$, **(d)** Non-dimensional Load vs Failure Index (Tsai-Wu criterion) for panel with $R/a = 5$

6.3.6 Effect of the shape of the cutout

In this section, the effect of the shape of the cutout on the stability and failure of a laminated composite cylindrical panel subjected to in-plane pulse load is investigated. A cylindrical panel with $R/a=10$, $b/a=1$, $b/h=100$, is considered. The panel is subjected to rectangular pulse load. The stacking sequence is $(0^\circ/90^\circ/90^\circ/0^\circ)$ and $(45^\circ/-45^\circ/-45^\circ/45^\circ)$. Three types of cutouts are considered for the study: circular, square and square-rotated. The plan of the three cutout shapes is shown in Fig. 3.9(a) - Fig. 3.9(c). Three cutout areas are considered: 5%, 10% and 20%.

Figure 6.12(a) shows the plot of non-dimensional load vs non-dimensional displacement for a panel having stacking sequence $(0^\circ/90^\circ/90^\circ/0^\circ)$ and 5% cutout area. Figure 6.12(b) shows the plot of the non-dimensional load vs non-dimensional displacement for a panel having stacking sequence $(0^\circ/90^\circ/90^\circ/0^\circ)$ and 10% cutout area. Figure 6.12(c) shows the plot of non-dimensional load vs non-dimensional displacement for a panel having stacking sequence $(0^\circ/90^\circ/90^\circ/0^\circ)$ and 20% cutout area. Figure 6.12(d) shows the plot of non-dimensional load vs failure index for a panel having stacking sequence $(0^\circ/90^\circ/90^\circ/0^\circ)$ and 5% cutout area. Figure 6.12(e) shows the plot of the non-dimensional load vs failure index for a panel having stacking sequence $(0^\circ/90^\circ/90^\circ/0^\circ)$ and 10% cutout area. Figure 6.12(f) shows the plot of non-dimensional load vs failure index for a panel having stacking sequence $(0^\circ/90^\circ/90^\circ/0^\circ)$ and 20% cutout area.

Figure 6.13(a) shows the plot of non-dimensional load vs non-dimensional displacement for a panel having stacking sequence $(45^\circ/-45^\circ/-45^\circ/45^\circ)$ and 5% cutout area. Figure 6.13(b) shows the plot of non-dimensional load vs non-dimensional displacement for a panel having stacking sequence $(45^\circ/-45^\circ/-45^\circ/45^\circ)$ and 10% cutout area. Figure 6.13(c) shows the plot of non-dimensional load vs non-dimensional displacement for a panel having stacking sequence $(45^\circ/-45^\circ/-45^\circ/45^\circ)$ and 20% cutout area. Figure 6.13(d) shows the plot of non-dimensional load vs failure index for a panel having stacking sequence $(45^\circ/-45^\circ/-45^\circ/45^\circ)$ and 5% cutout area. Figure 6.13(e) shows the plot of non-dimensional load vs failure index for a panel having stacking sequence $(45^\circ/-45^\circ/-45^\circ/45^\circ)$ and 10% cutout area. Figure 6.13(f) shows the plot of non-dimensional load vs failure index for a panel having stacking sequence $(45^\circ/-45^\circ/-45^\circ/45^\circ)$ and 20% cutout area. Panels in Fig. 6.12 and Fig. 6.13 are subjected to rectangular pulse loads.

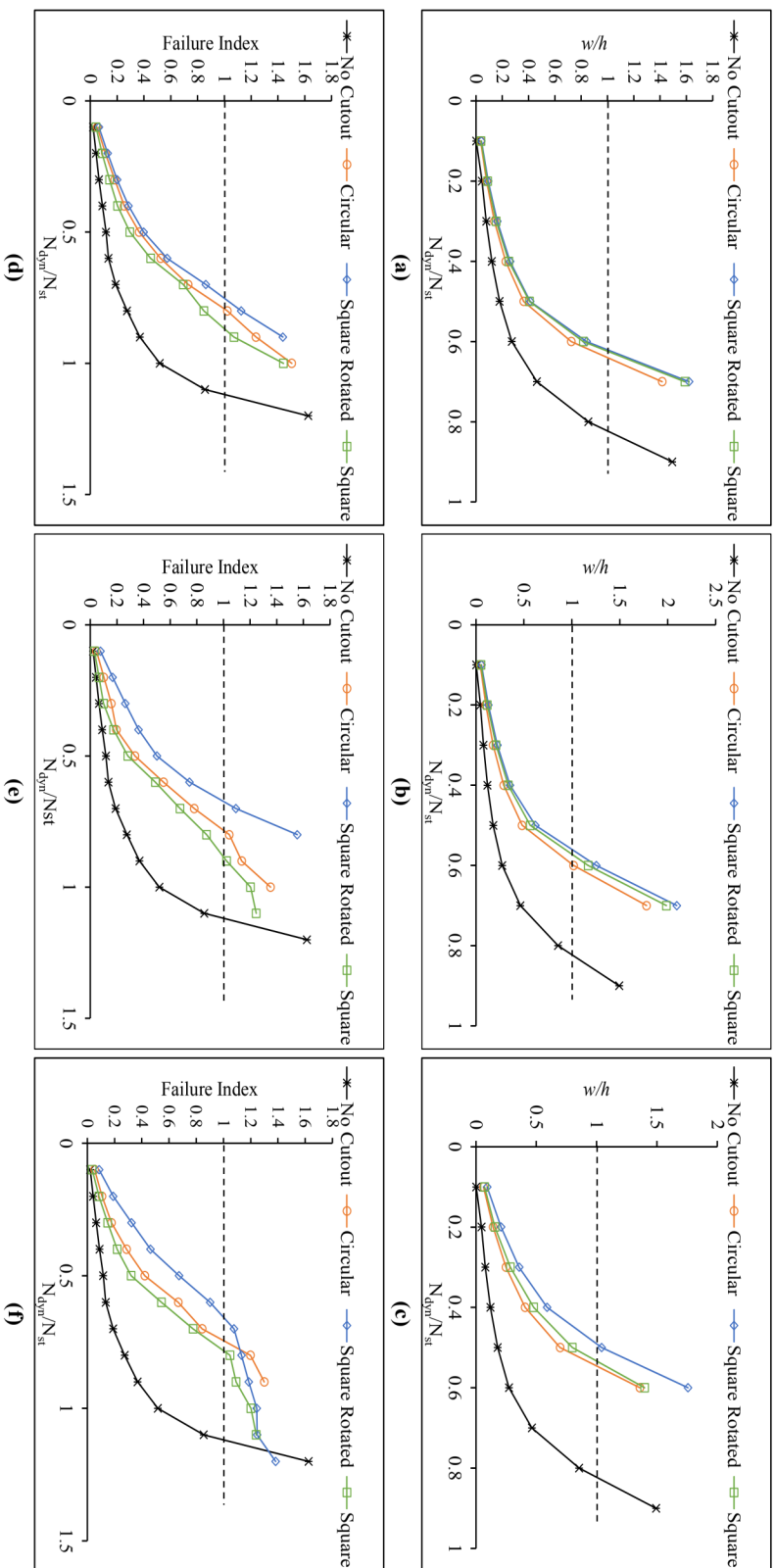


Fig. 6.12 Plot for a panel with $R/a=10$, $b/a=1$, $b/h=100$, stacking sequence $(0^\circ/90^\circ/90^\circ/0^\circ)$ and subjected to rectangular pulse load for various cutout shapes. **(a)** Non-dimensional Load vs non-dimensional Displacement for panel with 5% cutout area **(b)** Non-dimensional Load vs non-dimensional Displacement for panel with 10% cutout area **(c)** Non-dimensional Load vs non-dimensional Displacement for panel with 20% cutout area **(d)** Non-dimensional Load vs Failure Index for panel with 5% cutout area **(e)** Non-dimensional Load vs Failure Index for panel with 10% cutout area **(f)** Non-dimensional Load vs Failure Index for panel with 20% cutout area

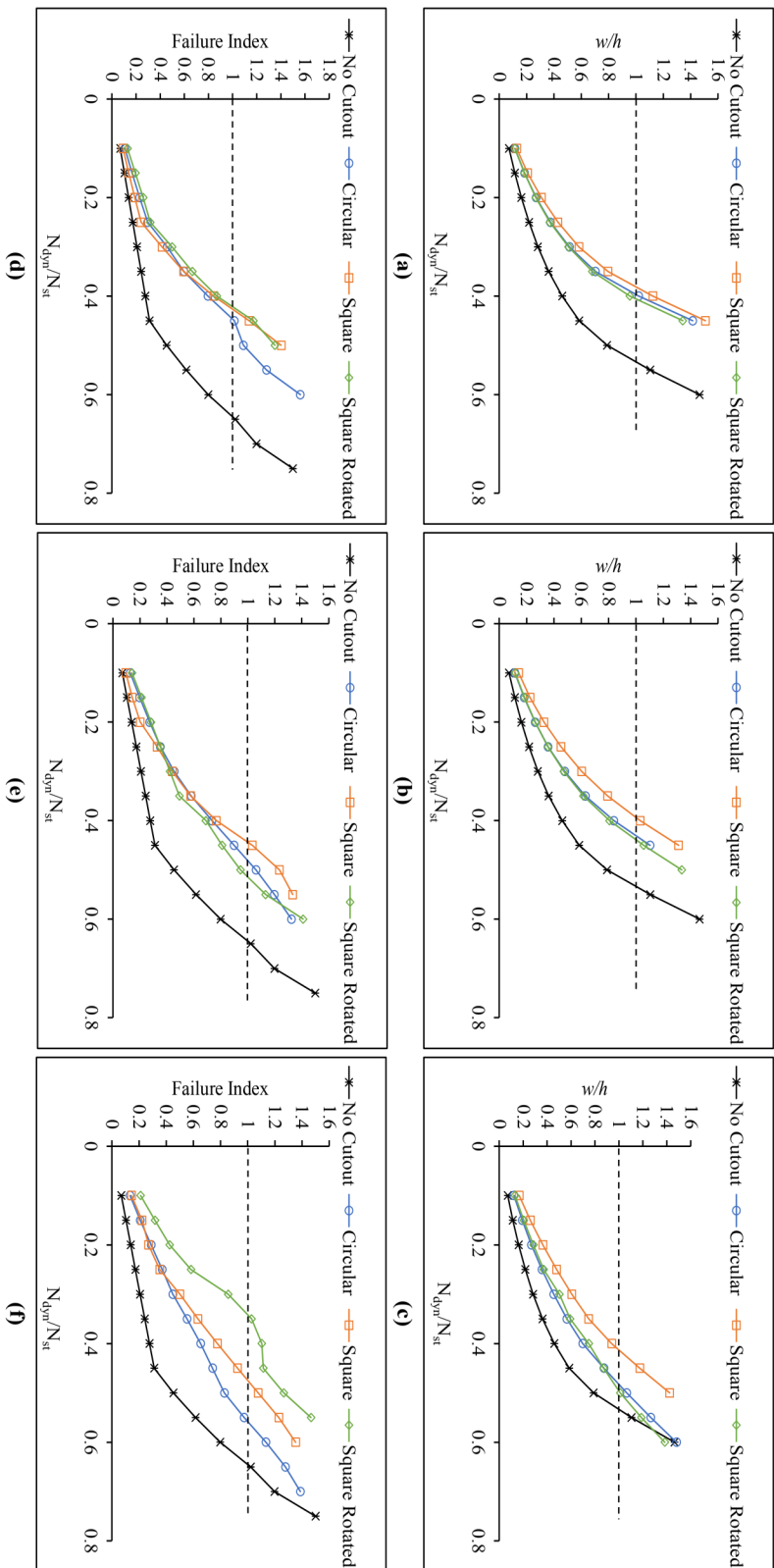


Fig. 6.13 Plot for a panel with $R/a=10$, $b/a=1$, $b/h=100$, stacking sequence (45°/-45°/45°/45°) and subjected to rectangular pulse load for various cutout shapes. **(a)** Non-dimensional Load vs non-dimensional Displacement for panel with 10% cutout area **(b)** Non-dimensional Load vs non-dimensional Displacement for panel with 5% cutout area **(c)** Non-dimensional Load vs non-dimensional Displacement for panel with 20% cutout area **(d)** Non-dimensional Load vs Failure Index for panel with 10% cutout area **(e)** Non-dimensional Load vs Failure Index for panel with 5% cutout area **(f)** Non-dimensional Load vs Failure Index for panel with 20% cutout area

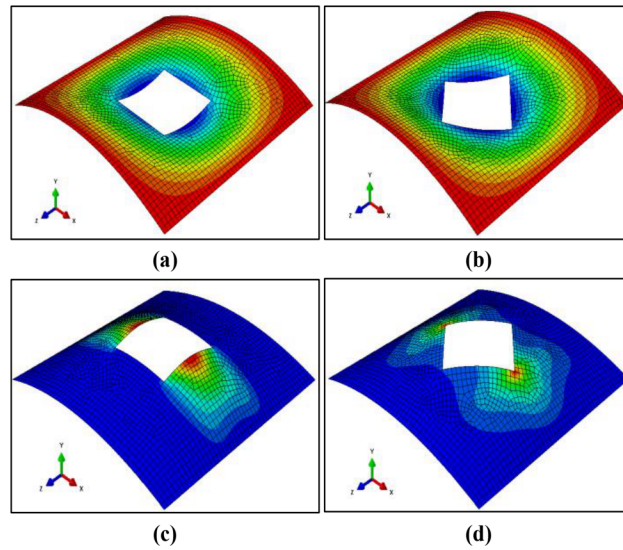


Fig. 6.14 Deformed shape of the panel with $R/a=10$, stacking sequence $(0^\circ/90^\circ/90^\circ/0^\circ)$, 10% cutout area and subjected to rectangular pulse load (a) $N_{dyn}/N_{st} = 0.6$ showing the maximum transverse displacement (b) $N_{dyn}/N_{st} = 0.6$ showing the maximum transverse displacement (c) $N_{dyn}/N_{st} = 0.9$ showing the failure index for Tsai-Wu criterion (d) $N_{dyn}/N_{st} = 0.7$ showing the failure index for Tsai-Wu criterion

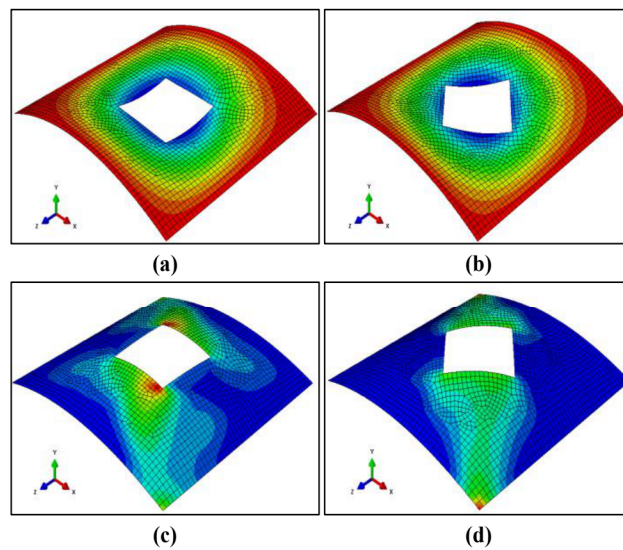


Fig. 6.15 Deformed shape of the panel with $R/a=10$, stacking sequence $(45^\circ/-45^\circ/-45^\circ/45^\circ)$, 10% cutout area and subjected to rectangular pulse load (a) $N_{dyn}/N_{st} = 0.4$ showing the maximum transverse displacement (b) $N_{dyn}/N_{st} = 0.45$ showing the maximum transverse displacement (c) $N_{dyn}/N_{st} = 0.45$ showing the failure index for Tsai-Wu criterion (d) $N_{dyn}/N_{st} = 0.55$ showing the failure index for Tsai-Wu criterion

In Fig. 6.12 and Fig. 6.13, the static buckling load (N_{st}) of each panel with different cutout shape and area of the cutout is different. In Fig. 6.12(a) the plot of the panel with 5% square cutout and the square-rotated cutout merge. However, the dynamic buckling load of the panel with square and square-rotated cutout is cutout is 38% lower than its corresponding static buckling load. The dynamic performance of the panel is compared with its own static buckling load.

It is observed from Fig. 6.12(a) the panel having cross-ply laminates with 5% circular, square and square-rotated cutout areas have dynamic buckling loads 36%, 38% and 39% lower than their respective static buckling loads. In Fig. 6.12 (d) for the panel having cross-ply laminates with 5% circular, square and square-rotated cutout areas, the first ply failure loads are 2%, 13% and 25% lower than their respective static buckling loads. It is observed from Fig. 6.12(b) the panel having cross-ply laminates with 10% circular, square and square-rotated cutout areas have dynamic buckling loads 40%, 42% and 44% lower than their respective static buckling loads. In Fig. 6.12 (e) for the panel having cross-ply laminates with 10% circular, square and square-rotated cutout areas, the first ply failure loads are 22%, 12% and 33% lower than their respective static buckling loads. It is observed from Fig. 6.12(c) the panel having cross-ply laminates with 20% circular, square and square-rotated cutout areas have dynamic buckling loads 45%, 47% and 51% lower than their respective static buckling loads. In Fig. 6.12 (f) for the panel having cross-ply laminates with 20% circular, square and square-rotated cutout areas, the first ply failure loads are 25%, 22% and 35% lower than their respective static buckling loads.

It is observed from Fig. 6.13(a) the panel having angle-ply laminates with 5% circular, square and square-rotated cutout areas have dynamic buckling loads 60%, 62% and 59% lower than their respective static buckling loads. In Fig. 6.12 (d) for the panel having angle-ply laminates with 5% circular, square and square-rotated cutout areas, the first ply failure loads are 47%, 54% and 55% lower than their respective static buckling loads. It is observed from Fig. 6.13(b) the panel having angle-ply laminates with 10% circular, square and square-rotated cutout areas have dynamic buckling loads 57%, 60% and 56% lower than their respective static buckling loads. In Fig. 6.13 (e) for the panel having angle-ply laminates with 10% circular, square and square-rotated cutout areas, the first ply failure loads are 52%, 56% and 49% lower than their respective static buckling loads. It is observed from Fig. 6.13(c) the panel having

angle-ply laminates with 20% circular, square and square-rotated cutout areas have dynamic buckling loads 52%, 58% and 52% lower than their respective static buckling loads. In Fig. 6.13 (f) for the panel having angle-ply laminates with 20% circular, square and square-rotated cutout areas, the first ply failure loads are 44%, 52% and 66% lower than their respective static buckling loads.

These results signify that the panels with cutouts have lower stiffness and strength when subjected to in-plane rectangular or sinusoidal pulse loads. In each case, the panel has lower dynamic buckling load and first ply failure load compared to its static buckling load when subjected to pulse load till its first natural period.

Figures 6.14(a)-6.14(d) show the deformed shape of the panel with $R/a = 10$ and stacking sequence $(0^\circ/90^\circ/90^\circ/0^\circ)$. Figures 6.15(a)-6.15(d) show the deformed shape of the panel with stacking sequence $(45^\circ/-45^\circ/-45^\circ/45^\circ)$. Both square and square-rotated cutouts are shown at critical time for maximum deformation at dynamic buckling load and first ply failure. Blue regions in Fig. 6.14(a), Fig. 6.14(b), Fig. 6.15(a) and Fig. 6.15(b) represent the area with maximum displacement. And the region in red in Fig. Fig. 6.14(c), Fig. 6.14(d), Fig. 6.15(c) and Fig. 6.15(d) represents the area with maximum failure index.

From these figures and Fig. 6.6 it is observed that the maximum displacement occurs near the cutout region. Also, with the change in stacking sequence, the region does not alter the deformation shape. However, a shift in the area where first ply failure occurs changes with the change in the stacking sequence in the panel.

6.3.7 Deformation of the cylindrical panel with a cutout

In this section, the deformation of a composite cylindrical panel with a cutout is presented. The deformed shapes of the panels at dynamic buckling loads are presented in previous sections, however, the deformation at various magnitude of loads is presented. Panel with $b/a=1$, $b/h=100$, $R/a=10$ and stacking sequence $(0^\circ/90^\circ/90^\circ/0^\circ)$ is considered. Three shapes of cutouts are considered: Circular, Square and Square-Rotated. The area of the cutout is 10% in each case.

Figure 6.16, 6.18 and 6.20 show the plot of non-dimensional load vs non-dimensional displacement for a panel with stacking sequence $(0^\circ/90^\circ/90^\circ/0^\circ)$ and 10% cutout area when

subjected to rectangular pulse load along with the deformed shapes of the panel at various magnitude of loads for circular, square and square-rotated cutouts respectively. Figure 6.17, 6.19 and 6.21 show the plot of non-dimensional load vs failure index with respect to Tsai-Wu failure criterion for panel with stacking sequence $(0^\circ/90^\circ/90^\circ/0^\circ)$ and 10% cutout area when subjected to rectangular pulse load along with the deformed shape of the panel at various magnitude of loads for circular, square and square-rotated cutouts respectively.

It is observed from Fig. 6.16 - Fig. 6.21 that the location of maximum deformation at various magnitude of loads does not change with the change in the shape of the cutout. The location of the maximum failure index is always at the cutout location. The scale factor for all these figures is kept 10.

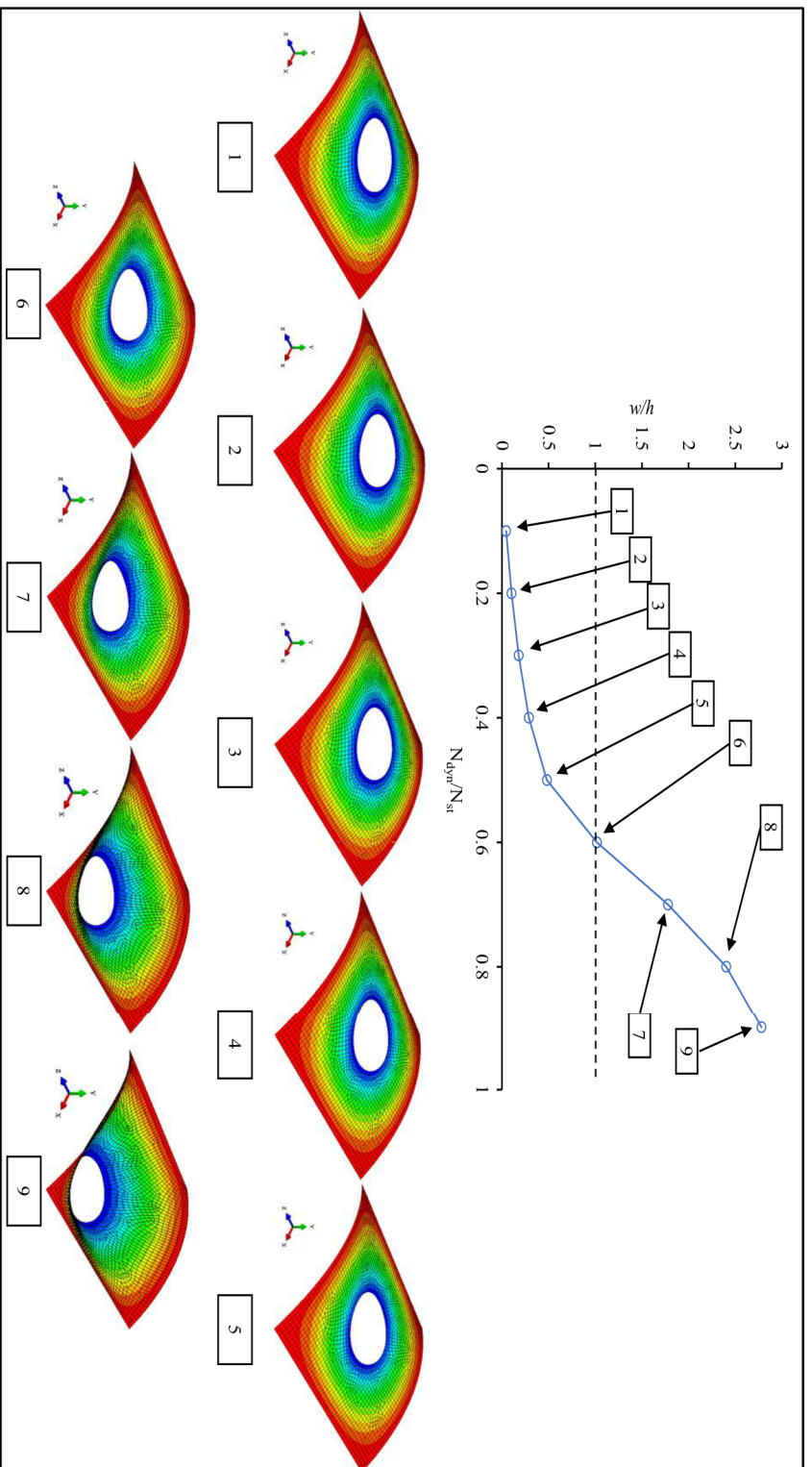


Fig. 6.16 Non-dimensional Load vs Displacement for a panel with $b/a=1$, $b/h=100$, $R/a=10$, stacking sequence ($0^\circ/90^\circ/90^\circ/0^\circ$) and 10% Circular cutout area when subjected to rectangular pulse load along with deformed shape of the panel at various magnitude of loads. Scale factor=10.

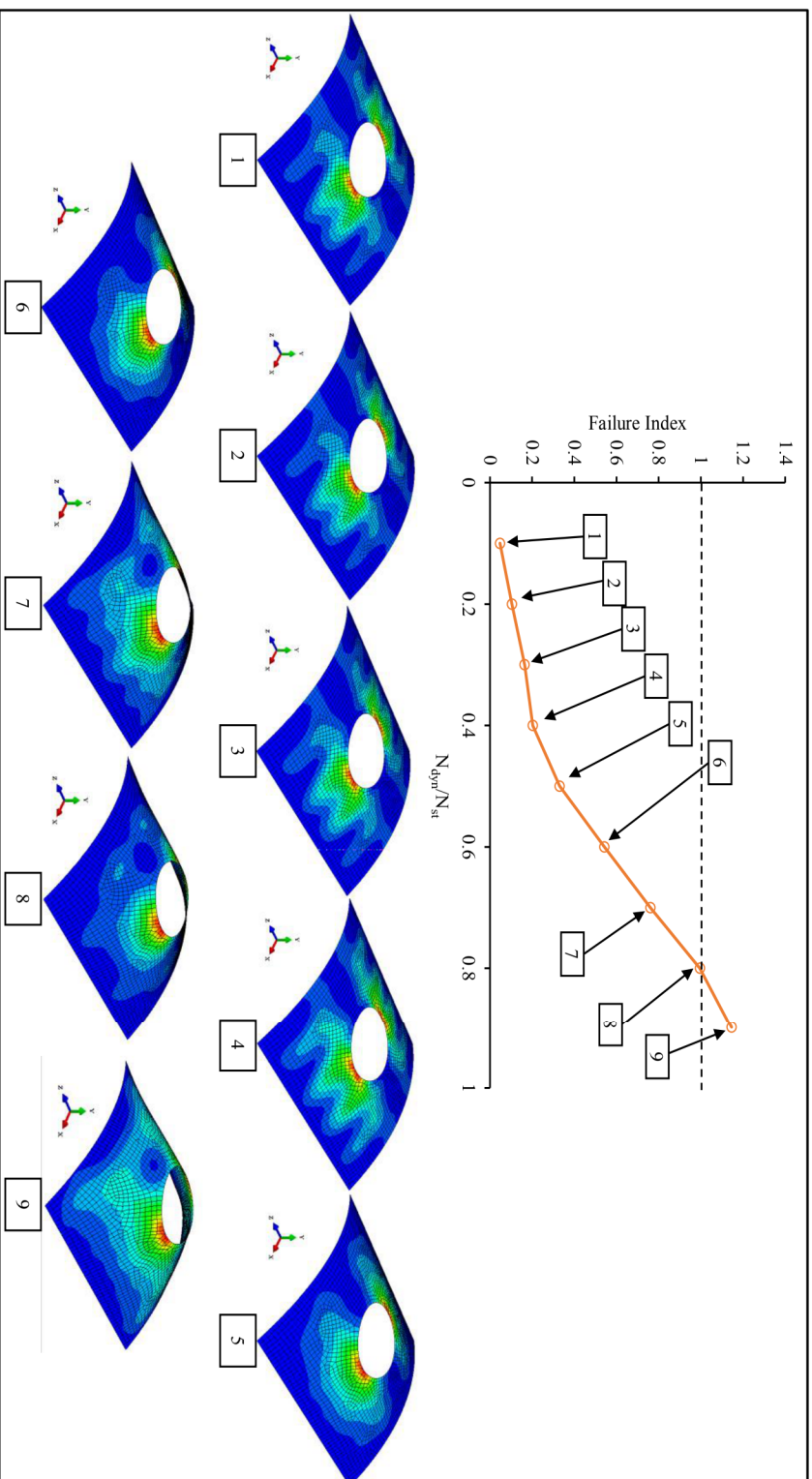


Fig. 6.17 Non-dimensional Load vs Failure Index (Tsai-Wu criterion) for a panel with $b/a=1$, $b/h=100$, $R/a=10$, stacking sequence ($0^\circ/90^\circ/90^\circ/0^\circ$) and 10% Circular cutout area when subjected to rectangular pulse load along with deformed shape of the panel at various magnitude of loads. Scale factor=10.

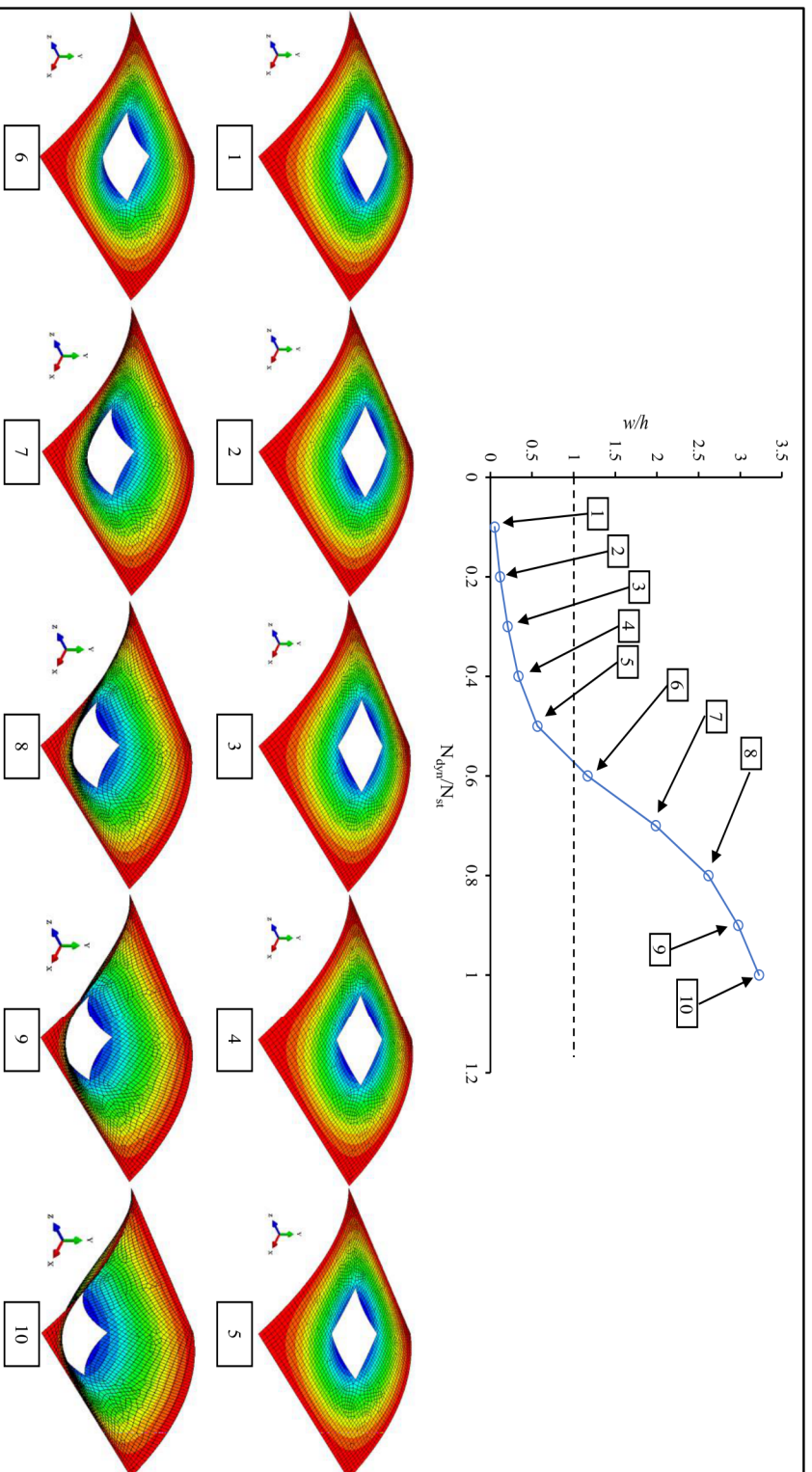


Fig. 6.18 Non-dimensional Load vs Displacement for a panel with $b/a=1$, $b/h=100$, $R/a=10$, stacking sequence $(0^\circ/90^\circ/90^\circ/0^\circ)$ and 10% Square cutout area when subjected to rectangular pulse load along with deformed shape of the panel at various magnitude of loads. Scale factor=10.

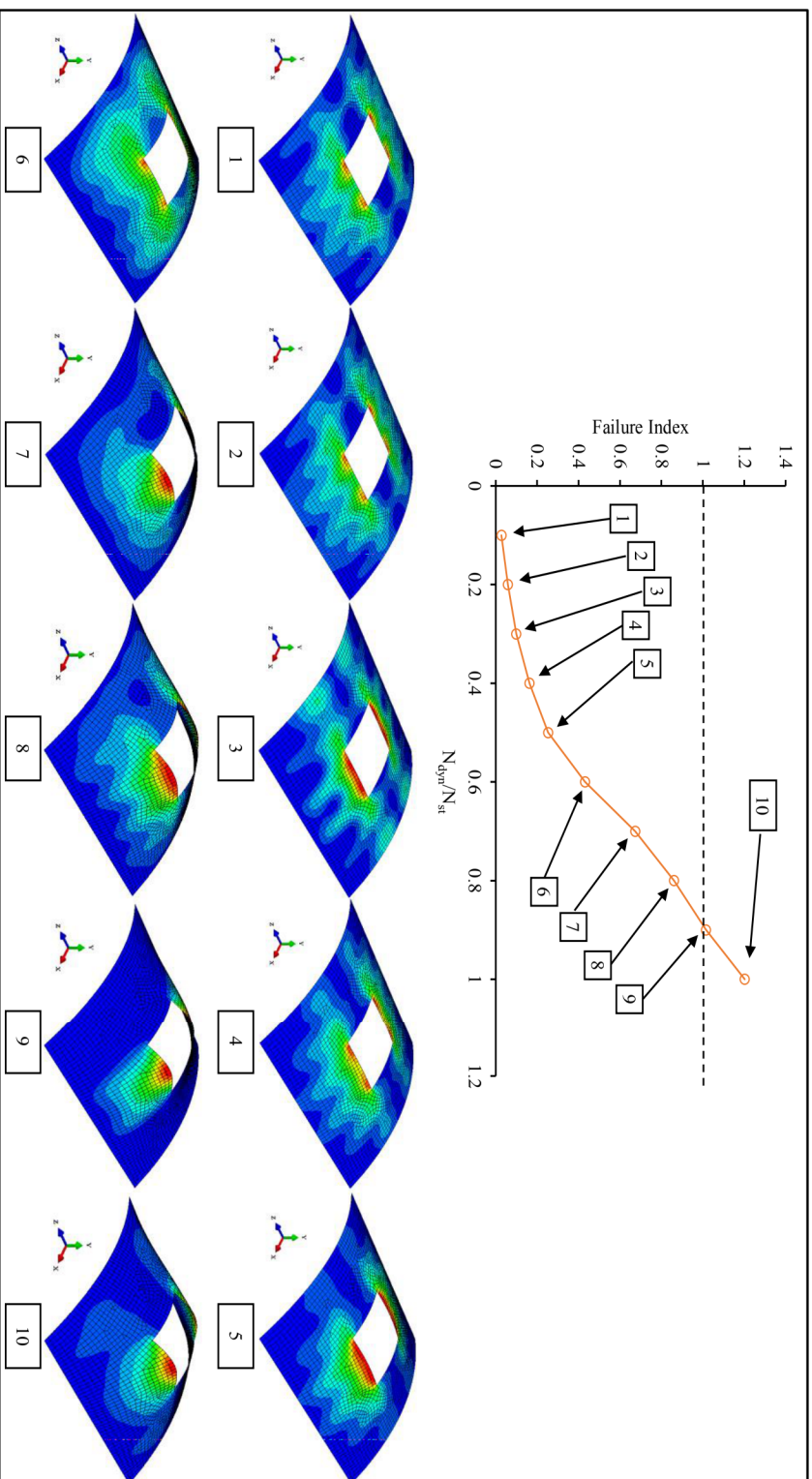


Fig. 6.19 Non-dimensional Load vs Failure Index (Tsai-Wu criterion) for a panel with $b/a=1$, $b/h=100$, $R/a=10$, stacking sequence $(0^\circ/90^\circ/90^\circ/0^\circ)$ and 100% Square cutout area when subjected to rectangular pulse load along with deformed shape of the panel at various magnitude of loads. Scale factor=10.

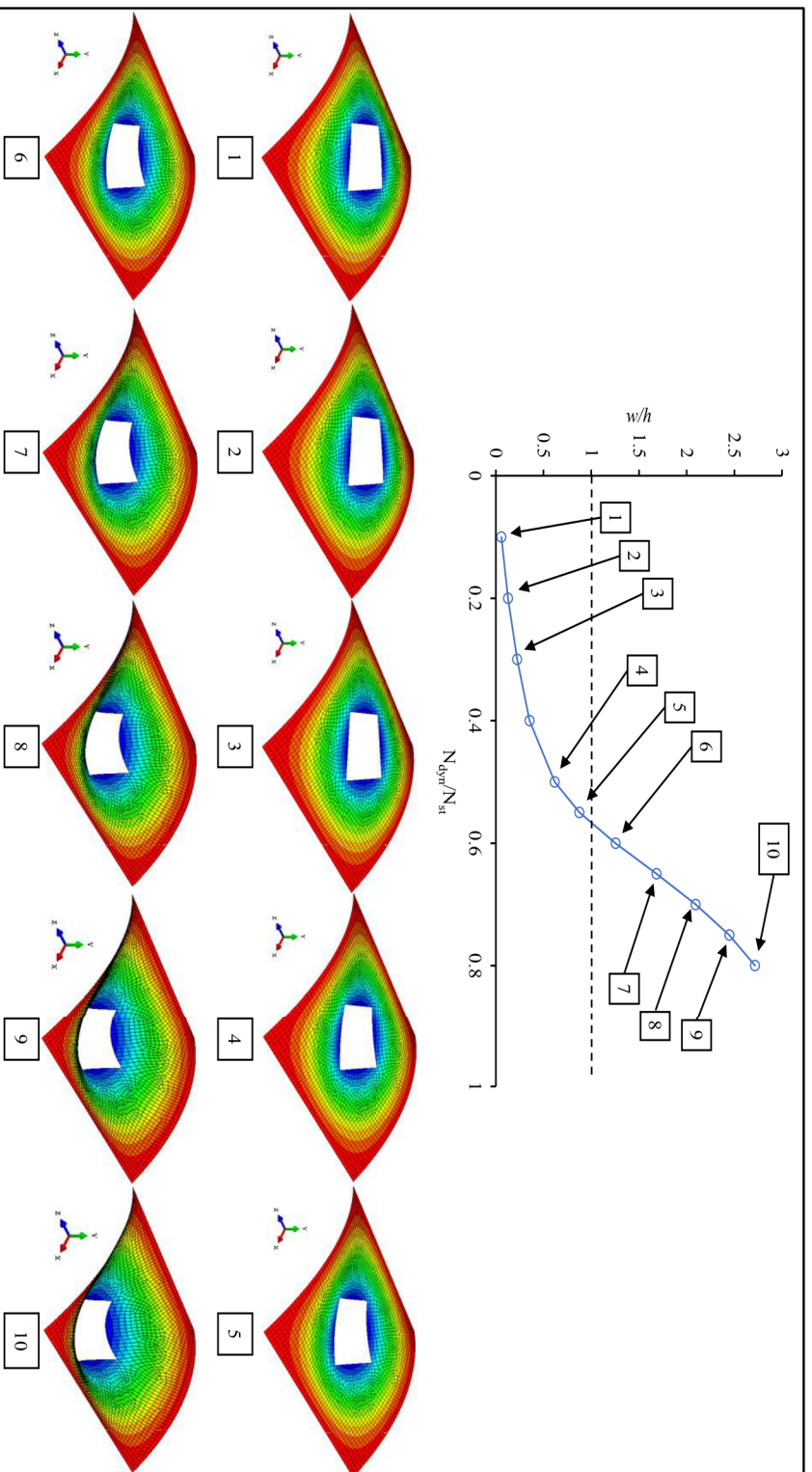


Fig. 6.20 Non-dimensional Load vs Displacement for a panel with $b/a=1$, $b/h=100$, $R/h=10$, stacking sequence $(0^\circ/90^\circ/90^\circ/0^\circ)$ and 10% Square-Rotated cutout area when subjected to rectangular pulse load along with deformed shape of the panel at various magnitude of loads. Scale factor=10.

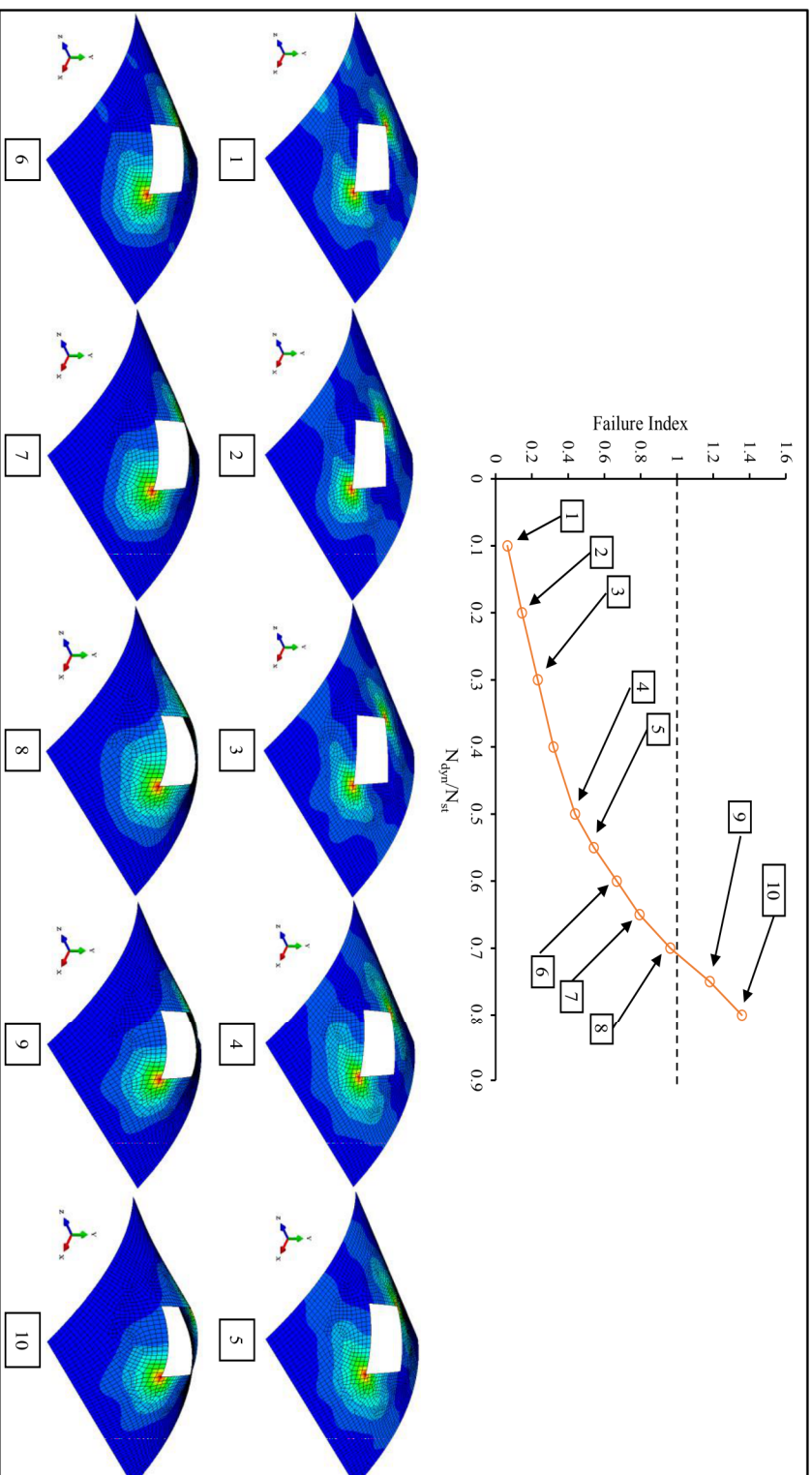


Fig. 6.21 Non-dimensional Load vs Failure Index (Tsaï-Wu criterion) for a panel with $b/a=1$, $b/h=100$, $R/a=10$, stacking sequence $(0^\circ/90^\circ/90^\circ/0^\circ)$ and 10% Square-Rotated cutout area when subjected to rectangular pulse load along with deformed shape of the panel at various magnitude of loads. Scale factor=10.

6.4 Summary

In this chapter, the non-linear dynamic buckling behaviour of a laminated composite cylindrical panel with a cutout is investigated. The influence of various parameters such as loading duration, stacking sequence, curvature of the panel, size and shape of cutouts on the dynamic buckling behaviour and the failure of the panel are also studied. The conclusions drawn from the study are presented in Chapter 8 (section 8.5).



This document was created with the Win2PDF "print to PDF" printer available at <http://www.win2pdf.com>

This version of Win2PDF 10 is for evaluation and non-commercial use only.

This page will not be added after purchasing Win2PDF.

<http://www.win2pdf.com/purchase/>